LAWRENCE
LIVERMORE
NATIONAL
LABORATORY

LLNL-CONF-656327

Predictions for p+Pb Collisions at sqrt{s} = 5 TeV: Expectations vs. Data

R. Vogt

July 1, 2014

Quark Matter 2014
Darmstadt, Germany
May 19, 2014 through May 24, 2014

Disclaimer

This document was prepared as an account of work sponsored by an agency of the United States government. Neither the United States government nor Lawrence Livermore National Security, LLC, nor any of their employees makes any warranty, expressed or implied, or assumes any legal liability or responsibility for the accuracy, completeness, or usefulness of any information, apparatus, product, or process disclosed, or represents that its use would not infringe privately owned rights. Reference herein to any specific commercial product, process, or service by trade name, trademark, manufacturer, or otherwise does not necessarily constitute or imply its endorsement, recommendation, or favoring by the United States government or Lawrence Livermore National Security, LLC. The views and opinions of authors expressed herein do not necessarily state or reflect those of the United States government or Lawrence Livermore National Security, LLC, and shall not be used for advertising or product endorsement purposes.

Available online at www.sciencedirect.com

ScienceDirect

Nuclear Physics A 00 (2014) 1–4

Nuclear Physics A

Predictions for p+Pb Collisions at $\sqrt{s_{NN}}$ = 5 TeV: Expectations vs. Data

R. Vogt (for the JET Collaboration)[1]

Physics Division, Lawrence Livermore National Laboratory, Livermore, CA 94551, USA
Physics Department, University of California, Davis, CA 95616, USA

Abstract

Recently a compilation of predictions for charged hadron, identified light hadron, quarkonium, photon, jet and gauge boson production in p+Pb collisions at $\sqrt{s_{NN}}$ = 5 TeV was made available [1]. Here the predictions are compared to the data so far available.

Keywords: cold nuclear matter effects, charged particle production, J/ψ

1. Introduction

Members and friends of the JET Collaboration calculated predictions for the $\sqrt{s_{NN}}$ = 5.02 TeV p+Pb run at the LHC in the winter of 2013. Predictions were collected for charged hadrons; identified particles; photons; jets; quarkonium; and gauge bosons. The observables included individual distributions, ratios such as $R_{p\mathrm{Pb}}$, and correlation functions. The predictions were compiled in Ref. [1]. This proceedings presents the confrontation of some of the predictions with data available at the time of this conference. We focus on charged hadron multiplicities and quarkonium here.

The charged particle multiplicities, p_T distributions and nuclear modification factors, $R_{p\mathrm{Pb}}$, in p+Pb collisions can be calculated in several different approaches. These are briefly outlined here. All involve some parameters tuned at a specific energy to predict results for other energies. For details and model references see Ref. [1].

Event generators determine multiplicities from their models of soft particle production followed by fragmentation and hadronization. Hard particle production is typically based on a pp generator such as `PYTHIA`. Examples include `HIJING`, `HIJINGB$\overline{\mathrm{B}}$` and `AMPT`.

Perturbative QCD approaches involving collinear factorization at leading and next-to-leading order typically require a minimum p_T to calculate the p_T distributions and modification factors. These calculations differ in the cold nuclear matter effects employed and the parameters used. Nuclear shadowing is generally included, as is isospin. Broadening of the p_T distributions in cold matter and medium-induced energy loss are also often included.

The color glass condensate (CGC) approach provides a saturation-based description of the initial state that can predict the total multiplicity. In this approach, gluon production can be described by k_{T}-factorization which assumes an ordering in intrinsic transverse momentum. The unintegrated gluon density associated with k_T factorization is related to the color dipole forward scattering amplitude which satisfies the JIMWLK evolution equations. In the

[1] A list of members of the JET Collaboration and acknowledgements can be found at the end of this issue.

large N_c limit, the JIMWLK equations simplify to the Balitsky-Kovchegov (BK) equation, a closed-form result for the rapidity evolution of the dipole amplitude. The running coupling corrections to the leading log BK equation, rcBK, have been phenomenologically successful in describing the rapidity/energy evolution of the dipole. The initial condition still needs to be modeled with parameters constrained by data. The impact parameter dependent dipole saturation model (IP-Sat) is a refinement of the dipole saturation model that reproduces the correct limit when the dipole radius $r_T \to 0$. It includes power corrections to the collinear DGLAP evolution and should be valid where logs in Q^2 dominate logs of x.

2. Charged Hadrons

In our compilation [1], it was shown that the charged particle pseudorapidity distributions, $dN_{\rm ch}/d\eta$, exhibited a considerably steeper slope than the data, particularly for η in the direction of the lead nucleus. Further communication with Albacete and Dumitru [11] showed that $dN_{\rm ch}/d\eta$ depends strongly on the $y \longrightarrow \eta$ transformation. The rcBK calculation depends on this Jacobian, not uniquely defined in the CGC framework. It is necessary to assume a fixed minijet mass, related to the pre-hadronization/fragmentation stage. Thus, in Ref. [1], they assumed the same transformation for pp and p+Pb collisions. If, instead, the hadron momentum is modified by $\Delta P(\eta) = 0.04\eta[(N_{\rm part}^{\rm proj} + N_{\rm part}^{\rm targ})2 - 1]$, the results are essentially identical in the proton direction but differ considerably in the direction of the lead beam [11]. The difference, bringing the calculation into better agreement with the data shows the sensitivity of this result to the mean mass and p_T of the unidentified final-state hadrons.

The left-hand side of Fig. 1 contrasts the centrality dependence of $dN_{\rm ch}/d\eta$ calculated with the default `AMPT` model [2] (smooth curves) and the b-CGC approach [3] (points with uncertainties). The calculations are in the same centrality bins as the ATLAS measurement [4]: 0-1%, 1-5%, 5-10%, 10-20%, 20-30%, 30-40%, 40-60%, 60-80% and 80-100%. There is no b-CGC result available for the 0-1% centrality bin.

In `AMPT`, the centrality in p+Pb collisions is defined according to the number of charged hadrons within $|\eta| < 1$ in the center of mass frame. The $40-60\%$ centrality bin gives a distribution that is very close to the min bias result, in particular on the proton side. The most central bin is the most asymmetric distribution, as well as the largest in magnitude. On the other hand, the distribution for the $80-100\%$ centrality bin is symmetric around $\eta_{\rm cm} = 0$.

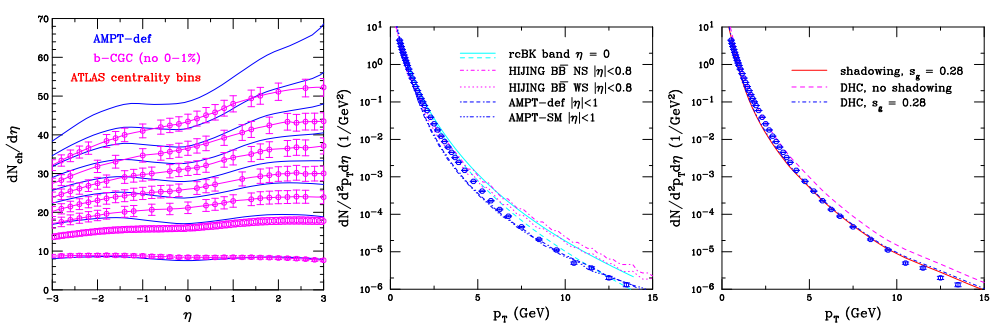

Figure 1: (Left) Charged particle pseudorapidity distributions in the center of mass frame of p+Pb collisions at various centralities for `AMPT` [2] and the b-CGC saturation model [3]. The calculations are in the same centrality bins as the ATLAS data [4]. (Center) Charged particle p_T distributions at $\sqrt{s_{NN}} = 5.02$ TeV. The solid and dashed cyan curves outline the rcBK band [5]. The magenta curves, calculated with `HIJINGBB̄2.0` are presented without (dot-dashed) and with (dotted) shadowing. The `AMPT` results are given by the dot-dash-dash-dashed (default) and dot-dot-dot-dashed (SM) blue curves. The data are from the ALICE Collaboration [6]. (Right) The charged hadron p_T distribution in p+Pb collisions with different `HIJING2.1` options is also compared to the ALICE data. All the calculations were presented in Ref. [1].

In the b-CGC approach [3], employing k_T factorization, the impact parameter dependence of the saturation model is crucial for defining the collision centrality. The asymmetry is largest in more central collisions while, for peripheral collisions such as the $60-80\%$ bin, the system becomes more similar to that of pp collisions. A fixed minijet mass equal to the current-quark mass is assumed. Since the minijet mass is related to pre-hadronization/hadronization

stage and cannot be obtained from saturation physics, it was fixed by fitting lower energy minimum-bias data. In very peripheral collisions, where the system becomes more similar to symmetric pp collisions, this assumption is less reliable. More importantly, k_T factorization is only proven in asymmetric pA collisions at small x. Thus this calculation is limited to $|\eta_{\rm cm}| \leq 3$.

The results of the two calculations are most similar in the more peripheral bins. The AMPT multiplicities tend to be slightly higher, especially in the lead (backward rapidity) direction. The b-CGC results have a somewhat more linear dependence on η and does not exhibit the dip at midrapidity seen in the AMPT calculations. The preliminary ATLAS centrality-dependent multiplicity [4] is somewhat higher in the direction of the proton beam (forward rapidity), especially in the most central (0-1%) bin.

The midrapidity, $|\eta| < 0.8$, charged hadron p_T distributions are shown in the center of Fig. 1 for rcBK [5], HIJINGB$\overline{\rm B}$2.0, and AMPT. The HIJINGB$\overline{\rm B}$2.0 distributions are similar to the rcBK results, albeit somewhat higher for $p_T > 10$ GeV/c. The AMPT distributions, on the other hand, drop faster at low p_T than the other results but then become harder at high p_T. The AMPT results are essentially independent of whether string melting is included or not while the HIJINGB$\overline{\rm B}$2.0 results without shadowing lie above those with shadowing. The right-hand side of Fig. 1 shows several options for cold matter effects in HIJING2.1 relative to $p + p$ collisions. The $p + p$ result is unscaled while the p+Pb curves with decoherent hard scatterings (DHC) without shadowing, DHC with shadowing, and shadowing only are separated from each other, starting from the $p + p$ result, by a factor of 100.

3. Quarkonium

The J/ψ and Υ results from ALICE [7, 8] and LHCb [9, 10] are in similar rapidity windows, $2.5 < y_{\rm cm} < 4$ for ALICE and $2.5 < y_{\rm cm} < 5$ for LHCb in symmetric (pp and AA) collisions. Although the muon spectrometers for both experiments are only on one side of the collision point, results were obtained forward and backward of midrapidity by switching the beam direction and running both p+Pb and Pb+p collisions. Due to the rapidity shift in asymmetric collisions, the acceptances of the two detectors in the collision center of mass was shifted to $2.03 < y_{\rm cm} < 3.53$ at forward rapidity and $-4.46 < y_{\rm cm} < -2.96$ at backward rapidity for ALICE and $1.5 < y_{\rm cm} < 4$ at forward rapidity and $-5 < y_{\rm cm} < -2.5$ at backward rapidity for LHCb. The regions of overlap between the forward and backward rapidity regions are $2.96 < |y_{\rm cm}| < 3.53$ for ALICE and $2.5 < |y_{\rm cm}| < 4$ for LHCb.

The results were presented first as $R_{p\rm Pb}(y)$, left-hand panel of Fig. 2, with an extrapolated pp normalization since there is no pp measurement at $\sqrt{s} = 5$ TeV. The pp normalization is based on an interpolation between the pp measurements at $\sqrt{s} = 2.76$ and 7 TeV, along with a model-based systematic uncertainty [7]. Note that ALICE presented both a single bin value of $R_{p\rm Pb}$ in the forward and backward regions as well as divided into six rapidity bins. In both rapidity regions, the ALICE points seem to be above the LHCb results. However, the data are compatible within the statistical uncertainties.

In addition, to eliminate the dependence on the uncertain pp normalization, a forward-backward production ratio, $R_{F/B}(y, \sqrt{s_{NN}}) = R_{p\rm Pb}(+|y|, \sqrt{s_{NN}})/R_{p\rm Pb}(-|y|, \sqrt{s_{NN}})$, was extracted where $R_{F/B}$ is defined with the proton beam moving toward positive y in the numerator and negative y in the denominator. Thus cold matter effects dominant at small x are in the numerator while the denominator probes larger x. The pp contributions to $R_{p\rm Pb}$ cancel in the ratio because pp collisions are symmetric around midrapidity. In both cases, the rapidity shift is taken into account to compare with calculations assuming no rapidity shift. The forward-backward ratio is shown as a function of rapidity and p_T in the center and right-hand panels of Fig. 2. The two measurements are in very good agreement within the region of overlap here, suggesting that the pp normalization is responsible for the difference seen in $R_{p\rm Pb}(y)$.

In addition to the J/ψ calculations in the color evaporation model (CEM) at next-to-leading order in Ref. [1], several other calculations are also shown.

The NLO EPS09 band is obtained by calculating the deviations from the central value for the 15 parameter variations on either side of the central set and adding them in quadrature (dashed histograms on the left-hand side of Fig. 2). The calculation was done the charm production parameters obtained in Ref. [14]. The EPS09 NLO band is narrower and exhibits less shadowing than the corresponding EPS09 LO CEM result.

The EPS09 LO CEM result is similar to that obtained in a LO color singlet model calculation [15] employing EPS09 LO. The band shown is the result of taking the EPS09 LO sets that give the minimum and maximum amount of gluon shadowing. The diffferences are not substantially due to the production model but to the mass and scale parameters employed.

The calculations by Arleo *et al.* are based on energy loss in cold nuclear matter, without and with the central EPS09 set. They fit an energy loss parameter, q_0, to the $\sqrt{s_{NN}}$ = 38.8 GeV E866 data and employ the same parameter for other energies. They find q_0 = 0.075 GeV^2/fm for the J/ψ without shadowing. The rapidity distributions modified by the energy loss probability, $P(\epsilon)$, used to fit q_0 are defined as $(1/A)(d\sigma_{pA}(y)/dy) = \int_0^{\min(E,E_p-E)} d\epsilon P(\epsilon)(E/(E+\epsilon))(d\sigma_{pp}(y+\delta y(\epsilon))/dy)$ where E is the energy of the quarkonium state in the rest frame of the nucleus. No specific quarkonium production model is assumed and instead a parameterization of the pp cross section, $d\sigma_{pp}/dp_T^2dx \propto [(1-x)^n/x][p_0^2/(p_0^2+p_T^2)]^m$, is adopted. The parameters n and m are fit to pp data. See Refs. [12, 13] for more details.

Finally, CGC calculations from Ref. [16] are also shown. The uncertainty comes from varying the saturation scale in the nucleus between 4 and 6 times that for the proton, $Q^2_{\mathrm{sat}A} \sim (4-6)Q^2_{\mathrm{sat}p}$, as well as varying the quark mass. The saturation scale is the biggest source of uncertainty.

The energy loss calculation agrees relatively well with the J/ψ data but underpredicts the Υ suppression. The CGC calculations overpredict the effect in the forward region but is closer to the Υ measurment. The EPS09 LO result is broad enough to encompass all the data while the smaller shadowing effect in EPS09 NLO underpredicts the results. With a consistent extraction of the gluon density at LO and NLO, the EPS09 LO and NLO CEM results should agree.

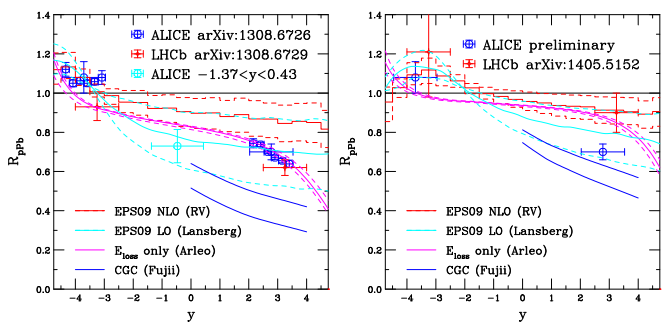

Figure 2: (Left) The $R_{p\mathrm{Pb}}$ ratio for J/ψ (left) and Υ (right) as a function of y. The red histogram shows the EPS09 NLO uncertainties [1] while the cyan curves show the EPS09 LO uncertainty as outlined by the minimum and maximum shadowing sets [15]. The magenta curves include energy loss only [12, 13]. Finally, the blue curves at forward rapidity are the result of a CGC calculation [16]. The ALICE [7, 8] and LHCb [9, 10] data are also shown.

I thank J. Albacete, F. Arleo, A. Dumitru, H. Fujii, F. Jing, J.-P. Lansberg, Z. Lin, A. Rezaeian, C. Roland, E. Scomparin, P. Steinberg, J. Velkovska, and X.-N. Wang for comments and contributions. This work was performed under the auspices of the U.S. Department of Energy by Lawrence Livermore National Laboratory under Contract DE-AC52-07NA27344 and supported in part by the JET collaboration.

References

[1] J. L. Albacete *et al*, Int. J. Mod. Phys. E **22** (2013) 1330007.
[2] Z.-W. Lin, C. M. Ko, B.-A. Li, B. Zhang and S. Pal, Phys. Rev. C **72** (2005) 064901.
[3] A. H. Rezaeian, Phys. Lett. B **718** (2013) 1058.
[4] R. Debbe *et al.* (ATLAS Collaboration), these proceedings.
[5] J. L. Albacete, A. Dumitru, H. Fujii and Y. Nara, Nucl. Phys. A **897** (2013) 1 [arXiv:1209.2001 [hep-ph]].
[6] B. Abelev *et al.* (ALICE Collaboration), Phys. Rev. Lett. **110** (2013) 082302.
[7] B. Abelev *et al.* (ALICE Collaboration), JHEP **1402** (2014) 073.
[8] J. Casstillo Castellanos (ALICE Collaboration), these proceedings.
[9] R. Aaij *et al.* (LHCb Collaboration), JHEP **1402** (2014) 072.
[10] R. Aaij *et al.* (LHCb Collaboration), arXiv:1405.5152.
[11] J. Albacete and A. Dumitru, private communication.
[12] F. Arleo and S. Peigné, JHEP **1303** (2013) 122.
[13] F. Arleo, R. Kolevatov, S. Peigné and M. Rustamova, JHEP **1305** (2013) 155.
[14] R. E. Nelson, R. Vogt and A. D. Frawley, Phys. Rev. C **87** (2013) 014908.
[15] E. G. Ferreiro, F. Fleuret, J. P. Lansberg and A. Rakotozafindrabe, Phys. Rev. C **88** (2013) 047901.
[16] H. Fujii and K. Watanabe, Nucl. Phys. A **915** (2013) 1.